Biochimica et Biophysica Acta 1848 (2015) 895–906

Contents lists available at ScienceDirect

Biochimica et Biophysica Acta

journal homepage: www.elsevier.com/locate/bbamem

Study of the putative fusion regions of the preS domain of hepatitis B virus

Carmen L. Delgado [a,1], Elena Núñez [a,2], Belén Yélamos [a], Julián Gómez-Gutiérrez [a], Darrell L. Peterson [b], Francisco Gavilanes [a,*]

[a] Departamento de Bioquímica y Biología Molecular, Facultad de Ciencias Químicas, Universidad Complutense, 28040 Madrid, Spain
[b] Department of Biochemistry and Molecular Biology, Medical College of Virginia, Virginia Commonwealth University, Richmond, 23298 VA, USA

ARTICLE INFO

Article history:
Received 15 October 2014
Received in revised form 1 December 2014
Accepted 22 December 2014
Available online 29 December 2014

Keywords:
Fusion protein
HBV
Hepatitis virus
Membrane fusion
Protein domain
Phospholipid vesicle

ABSTRACT

In a previous study, it was shown that purified preS domains of hepatitis B virus (HBV) could interact with acidic phospholipid vesicles and induce aggregation, lipid mixing and leakage of internal contents which could be indicative of their involvement in the fusion of the viral and cellular membranes (Núñez, E. et al. 2009. Interaction of preS domains of hepatitis B virus with phospholipid vesicles. Biochim. Biophys. Acta 17884:417–424). In order to locate the region responsible for the fusogenic properties of preS, five mutant proteins have been obtained from the preS1 domain of HBV, in which 40 amino acids have been deleted from the sequence, with the starting point of each deletion moving 20 residues along the sequence. These proteins have been characterized by fluorescence and circular dichroism spectroscopy, establishing that, in all cases, they retain their mostly non-ordered conformation with a high percentage of β structure typical of the full-length protein. All the mutants can insert into the lipid matrix of dimyristoylphosphatidylglycerol vesicles. Moreover, we have studied the interaction of the proteins with acidic phospholipid vesicles and each one produces, to a greater or lesser extent, the effects of destabilizing vesicles observed with the full-length preS domain. The ability of all mutants, which cover the complete sequence of preS1, to destabilize the phospholipid bilayers points to a three-dimensional structure and/or distribution of amino acids rather than to a particular amino acid sequence as being responsible for the membrane fusion process.

1. Introduction

Hepatitis B virus (HBV) is a small DNA virus which infects the liver. Although infection is usually followed by a complete recovery, in some cases the infection becomes chronic and may result in the development of cirrhosis and hepatocellular carcinoma. HBV infection is still a worldwide health problem despite the fact that an effective vaccine has been available for more than 25 years. About 240 million people are chronic carriers of HBV and about 1 million become infected yearly [1].

HBV envelope proteins are involved in the binding of the virus to the hepatocytes and in the cell entry mechanism [2]. There are three surface proteins designated as the small (S), medium (M) and large (L), that are the product of a single open reading frame. They share 226 amino acids (full-length S protein) at the C-terminus. The M protein has an extension of 55 amino acids, preS2, at the N-terminus of the S. The L protein is composed of the entire M protein and the preS1 region at the N-terminus which has 108–119 amino acids, depending on the HBV genotype. The regions preS1 and preS2 together are known as preS domains [3].

The preS domains are functional at different steps of the virus life cycle. Several studies have demonstrated that preS1, and not preS2, contains the main hepatocyte specific binding domain [4], specifically a region from 21 to 47 residues [5–9]. Other studies indicate that the full-length preS1 domain, with the exception of amino acids 78 to 87, is essential for the infectivity of HBV [10] and the species specificity has been attributed to the first 30 amino acids of preS1 (subtype ayw) [11]. It is also widely accepted that myristoylation at Gly2 residue of the preS1 domain plays an important role in specific binding to hepatocytes [3,12–14]. Several molecules have been proposed to play a role in binding of HBV to hepatocytes [3,15–17]. Very recently sodium

Abbreviations: HBV, Hepatitis B Virus; NBD-PE, N-(7-nitro-2,1,3-benzoxadiazol-4-yl)-dimyristoylphosphatidylethanolamine; Rh-PE, N-(lissamine rhodamine B sulfonyl)-diacylphosphatidylethanolamine; DMPG, dimyristoylphosphatidylglycerol; ANTS, 8-Aminonaphtalene-1,3,6-trisulfonic acid; DPX, p-xylenebis(pyridinium) bromide; NBD-F, 4-fluoro-7-nitrobenz-2-oxa-1,3-diazole, IPTG, isopropyl-D-thiogalactopiranosyde; CCA, Convex Constraint Analysis

* Corresponding author. Tel.: +34 91 3944266; fax: +34 91 3944159.
E-mail address: pacog@bbm1.ucm.es (F. Gavilanes).
[1] Present address: ASICI Pabellón Central, Recinto Ferial, 06300 Zafra, Badajoz, Spain.
[2] Present address: Janssen-Cilag, S.A., Paseo de las Doce Estrellas, 5-7, 28042 Madrid, Spain.

http://dx.doi.org/10.1016/j.bbamem.2014.12.020
0005-2736/

taurocholate cotransporting polypeptide has been identified as a HBV cellular receptor [18].

Little is known about the involvement of the envelope proteins in the fusion between the viral and the host cell membrane. A peptide comprising the 16 amino acids at the N-terminal end of S protein have been shown to interact with model membranes, causing liposome destabilization in a pH-dependent manner and adopting an extended conformation during the process [19,20]. Evidence for the role of the N-terminal S peptide in woodchuck hepatitis B virus (WHV) or duck hepatitis B virus (DHBV) infectivity has also been obtained by others researchers [21,22]. On the other hand, we have previously shown that isolated preS domains (subtypes adw and ayw) are able to interact with acidic phospholipids vesicles and, as a result of this interaction, cause the destabilization of the bilayer, both at neutral and acidic pH [23]. Furthermore, the addition of this type of phospholipid vesicles led to a conformational change in the preS domain, increasing its helical content [23]. Similar results were obtained with the DHBV preS domain, despite the difference in the amino acid sequence [24]. Both domains share a similar hydrophobic profile, indicating that a three-dimensional conformation rather than a particular amino acid sequence would be responsible for the properties observed [24]. These results point to the possibility that both S and preS regions could contribute to the fusion of the viral and cellular membranes. Moreover, it has been shown that the preS2 domain plays an important role in virus assembly but it is dispensable in virus entry [25].

With the aim to locate the region of the preS domains responsible for the fusogenic properties, five deletion mutants along the preS1 sequence (subtype ayw) have been prepared. In each mutant, 40 amino acids were deleted, with the starting point of each deletion moving 20 residues along the sequence. Thus, the mutants are designated $preS_{\Delta1-40}$, $preS_{\Delta20-60}$, $preS_{\Delta40-80}$, $preS_{\Delta60-100}$ and $preS_{\Delta80-120}$, indicating the deleted region in each case. All the proteins were characterized spectroscopically, and their interaction with phospholipids was studied.

2. Materials and methods

2.1. Enzymes and reagents

Restriction enzymes, ligases, DNA polymerase and other molecular biology reagents were obtained from New England Biolabs, Promega, Invitrogen, Novagen or BRL. N-(7-nitro-2,1,3-benzoxadiazol-4-yl)-dimyristoylphosphatidylethanolamine (NBD-PE), N-(lissamine rhodamine B sulfonyl)-diacylphosphatidylethanolamine (Rh-PE) and dimyristoylphosphatidylglycerol (DMPG) were provided by Avanti Polar Lipids. 8-Aminonaphtalene-1,3,6-trisulfonic acid (ANTS), p-xylenebis(pyridinium) bromide (DPX) and 4-fluoro-7-nitrobenz-2-oxa-1,3-diazole (NBD-F) were purchased from Molecular Probes. Triton X-100 was obtained from Boehringer Mannheim. Sepharose CL-6B Ni-nitrilotriacetic acid (NTA) was purchased from Qiagen. All other reagents were obtained from Merck and Sigma. All solvents were of HPLC grade.

2.2. Cloning of preS-his and $preS_{\Delta1-40}$

To clone the preS domain (subtype ayw) and the $preS_{\Delta1-40}$ deletion mutant in the plasmid pT7-7 (Gibco BRL), the plasmid pET3d-preS-his-ayw [26], which contains the full-length preS domain (subtype ayw) followed by a region encoding a six-histidines tag at the carboxy-terminal end, was used as template. The forward primers used were preS-*Nde*I(+): 5-′GGA GAT ATA CAT ATG GGG CAG AAT C and Δ1-40-*Nde*I(+): 5′C AAC AAG CAT ATG TGG CCA GAC GC; the reverse primer for both cloning was preS-*Hind*III(-): 5′-GCA GCC AAG CTT CTA CTA ATG GTG. Underlined are the *Nde*I and *Hind*III restriction sites included in the primers.

The PCR reaction conditions were: 1 min at 94 °C, followed by five cycles at 94, 60 and 72 °C, each for 1 min, by 30 cycles at 94, 55 and 72 °C, each for 1 min, and a final "filling in" step at 72 °C for 7 min. The fragment of amplified DNA was purified by Wizard PCR Prep system (Promega) and was subcloned into the linear plasmid pCR2.1 (Invitrogen), with 3′T ends and ampicillin resistance gene. pCR2.1-preS and pT7-7 plasmids were subsequently digested with restriction enzymes *Nde*I (Boehringer Mannheim, 10 U/μL) and *Hind*III (New England Biolabs, 20 U/μL), in a final volume of 10 μL at room temperature for 16 h. After digestion, a 1% agarose gel was run. Once the suitable fragments had been copurified, using the QIAEX system (QIAGEN), they were ligated with bacteriophage T4 DNA ligase (Gibco BRL, 1 U/μL), at room temperature for 1-2 h, and *Escherichia coli* DH5αF′ cells were transformed with half of the reaction mixture. The positive colonies were identified by digestion of purified plasmid DNA with the restriction enzymes *Nde*I and *Hind*III. The individual cDNA sequences were confirmed by automated DNA sequencing. The resulting recombinant plasmids were called pT7-7-preS and pT7-7-Δ1-40.

2.3. Cloning of $preS_{\Delta20-60}$, $preS_{\Delta40-80}$, $preS_{\Delta60-100}$ and $preS_{\Delta80-120}$

The rest of the mutant cDNAs were obtained by the method described by Pogulis [27]. Briefly, the regions on both sides of the deletion were amplified separately by PCR, using the plasmid pT7-7-preS as template. Internal primers of each mutant had a complementary region of 18 nucleotides, corresponding to the 9 final nucleotides and the first 9 nucleotides located before and after the deletion. The conditions of this first PCR reaction were the same as described above for preS and $preS_{\Delta1-40}$. After running the PCR product on a 1.75% agarose gel and copurifying both regions using the QIAEX system (QIAGEN), a second elongation PCR using Taq Gold polymerase was carried out without primers in order to expand the area. The PCR conditions were: 15 cycles at 94, 52 and 72 °C, each for 1 min, followed by 7 min at 72 °C.

Finally, a third PCR using the amplified sequences as template, and the oligonucleotides preS-*Nde*I(+) and preS-*Hind*III(-) as primers, resulted in a DNA fragment with a region of 120 nucleotides deleted and 3′A ends. The PCR conditions were: 32 cycles at 94, 55 and 72 °C, each for 1 min, followed by a final step of 7 min at 72 °C. Then, they were cloned into the pCR2.1 plasmid, digested with restriction enzymes *Nde*I and *Hind*III and subsequently cloned into the plasmid pT7-7 digested with the same enzymes. The sequences of the different genes were confirmed by automated DNA sequencing.

2.4. Expression and purification of preS-his and deletion mutants

pT7-7 recombinant plasmids with the preS-his domain or the different deletion mutants were used to transform *E. coli* HMS174 (DE3) cells. In all cases, the expression of the recombinant protein was under the control of the T-7 promoter, inducible by isopropyl-D-thiogalactopiranosyde (IPTG).

A single colony was used to inoculate 50 mL of M9 medium supplemented with 0.17% glucose, 1.06 mM $MgSO_4$, 0.053 mM $CaCl_2$ and 100 μg/mL ampicillin. Following overnight incubation at 37 °C, the culture was used to inoculate 950 mL of the same medium. This culture was grown to an optical density at 600 nm of 0.6 and the IPTG was added to a final concentration of 0.5 mM, and incubated at 37 °C for 4 h to induce protein expression. Cells were harvested by centrifugation at 7400 g for 10 min in a GS-3 rotor (Sorvall). The cell pellet was resuspended in ice cold 10 mM MOPS pH 8.0, 10 mM imidazole, 0.3 M NaCl, 6 M Urea to avoid proteolytic degradation of proteins. Cells were lysed by sonication and centrifuged at 89500 g for 30 min in a Beckman SW-28 rotor.

Recombinant proteins were purified using a single affinity chromatography step in Sepharose CL-6B Ni-nitrilotriacetic acid (NTA)-agarose column (Qiagen) equilibrated with 10 mM MOPS pH 8.0, 10 mM imidazole, 0.3 M NaCl, 6 M Urea. After washing the non-specifically bound proteins with 10 mM MOPS pH 8.0, 30 mM imidazole, 6 M Urea, elution of the proteins was performed with 10 mM MOPS pH 8.0, 200 mM

imidazole, 6 M Urea. The urea was removed by dialysis against 10 mM MOPS pH 7.0. The presence of the different proteins was monitored through the purification by SDS-PAGE. The amino acid composition and the protein concentration were determined on a Beckman 6300 automatic amino acid analyzer.

2.5. Spectroscopic characterization of preS-his proteins

The far-UV circular dichroism spectra were recorded on a Jasco J-715 spectropolarimeter equipped with a thermostated cell. The protein concentration was 0.1 mg/mL. The buffer used was 10 mM MOPS, pH 7.0 or pH 5.0. A minimum of three spectra were accumulated for each sample and the contribution of the buffer was subtracted. Values of mean residue ellipticity were calculated on the basis of 110 as the average molecular mass per residue and they are reported in terms of $[\theta]_{M.R.W.}$ (degrees $\times$ cm^2 $\times$ $dmol^{-1}$). The secondary structure of each protein was evaluated by computer fit of the dichroism spectra according to the algorithm convex constraint analysis (CCA) [28]. This method relies on an algorithm that calculates the contribution of the secondary structure elements that give rise to the original spectral curve without referring to spectra from model systems.

Fluorescence studies were performed on a SLM Aminco 8000C spectrofluorimeter fitted with a 450 W Xenon lamp. The slits were set at 4 nm and the integration time was 1 s. The protein concentration was always 0.05 mg/mL. The buffer used was 10 mm MOPS, pH 5.0 or 7.0. At least three spectra were accumulated and the contribution of the buffer was subtracted. Excitation was performed at a wavelength of 275 or 295 nm, and emission spectra measured over a range of 285–465 nm. The tyrosine contribution to the emission spectra was calculated by subtracting from the emission spectra measured at $\lambda_{exc} = 275$ nm the emission spectra measured at $\lambda_{exc} = 295$ nm multiplied by a factor that was obtained from the ratio between the fluorescence intensities measured with $\lambda_{exc} = 275$ nm and $\lambda_{exc} = 295$ nm at wavelengths higher than 380 nm, where there is no tyrosine contribution.

2.6. Labeling of preS-his proteins

Fluorescent labeling of the N-terminus of the protein was achieved by the procedure of Rapaport and Shai [29] as previously described [24]. Some NBD-labeled proteins precipitated in the column. In these cases, the protein was denatured with 6 M Urea. The denaturant and the excess label reagent were removed by exhaustive dialysis against 10 mM MOPS pH 5.0 or 7.0, with decreasing concentrations (1, 0.5, 0.2, 0.1 and 0 M) of Urea.

2.7. Vesicle preparation

The vesicles used were prepared by sonication and extrusion in a Liposo Fast-Basic extruder apparatus (Avestin, Inc.) with 100-nm polycarbonate filters (Costar) as previously described [24].

2.8. Binding assay

The binding of NBD-preS-his or NBD-mutant proteins to PG vesicles was studied as previously described [24]. Briefly, after incubation of the protein (0.03–0.06 μM) with the vesicles for 1–2 min, the fluorescence spectra were taken between 480 and 650 nm with the excitation wavelength set at 467 nm in a SLM AMINCO 8000C spectrofluorimeter (SLM Instruments). The fluorescence intensity registered at 530 nm at different lipid/protein molar ratios was utilized to obtain the binding isotherm. The data were analyzed using the equation:

$$X_b^* = K_p^* \cdot C_f$$

where X_b^* is the molar ratio of bound protein per total lipid corrected taking into account that proteins only partitioned over the outer leaflet of vesicles ($X_b^* = X_b / 0.6$), K_p^* corresponds to the corrected partition coefficient and C_f represents the equilibrium concentration of free protein in solution. At every phospholipid concentration, the fraction of bound protein can be calculated by the formula:

$$f_b = (F - F_0)/(F_\infty - F_0)$$

where F_0 represents the fluorescence of unbound protein and F_∞ the fluorescence of bound protein. In all cases, fluorescence from control vesicles in the absence of labeled protein was subtracted. At least three different experiments were performed for each condition.

2.9. Vesicle aggregation

The aggregation of phospholipid vesicles induced by the addition of preS-his and mutant proteins was followed by measuring the optical density at 360 nm (ΔOD_{360}) on a Beckman DU-7 spectrophotometer [24]. The final phospholipid concentration was kept at 60 μM. At least three different experiments were performed for each condition.

2.10. Lipid mixing

The fluorescent probe dilution assay [30] was employed to determine lipid mixing. All the conditions are coincident with those previously used for human and duck preS proteins [23]. The energy transfer efficiency was calculated from the ratio of the emission intensities at 530 and 590 nm and the appropriated calibration curve.

2.11. Release of aqueous contents

The integrity of the phospholipid vesicles was assessed by the ANTS/DPX leakage assay [31] as previously described [23]. ANTS and DPX were co-encapsulated in phospholipid vesicles at 12.5 mM and 45 mM respectively, in 10 mM Tris pH 7.2, 20 mM NaCl. The non-encapsulated material was eliminated by chromatography in a Sephadex G-75 column (Pharmacia). The phospholipid concentration was kept at 0.1–0.14 mM. The fluorescence spectra were measured in a SLM Aminco 8000C spectrofluorimeter. The excitation wavelength was set at 385 nm and the ANTS emission was monitored at 520 nm. The fluorescence of control vesicles without protein was taken as 0% leakage while 100% was considered upon addition of 0.5% Triton X-100.

3. Results

3.1. Expression and purification

After inducing the expression of the preS and mutants with IPTG, the recombinant proteins were purified as described in the Materials and methods section. The results of the purification steps of preS-his are shown in Fig. 1A as an example. Induction with IPTG resulted in the appearance of a band which corresponded to the molecular mass of the preS-his domain (Fig. 1A, lanes 2 and 3). After lysis of the cells all the protein remained soluble (Fig. 1A, lane 5). Moreover, when loaded onto the Ni-NTA column most of the protein was retained (Fig. 1A, lane 6). The proteins were eluted with 10 mM MOPS pH 8.0, 200 mM imidazole, 0.3 M NaCl, 6 M urea. All proteins were homogeneous as it is shown by SDS-PAGE (Fig. 1B), with an electrophoretic mobility corresponding to that expected according to their molecular mass (Table 1), except for preS $_{\Delta 40-80}$, which has a lower mobility (Fig. 1B, lane 5). Moreover, their purity was higher than 98% in every case. Under these conditions, 15 mg per liter of cell culture of preS-his and about 3–6 mg of the different mutants were obtained.

The amino acid composition of the purified proteins was practically coincident with that expected from the cDNA sequence (Table 2), indicating the purity of the sample. The most significant difference

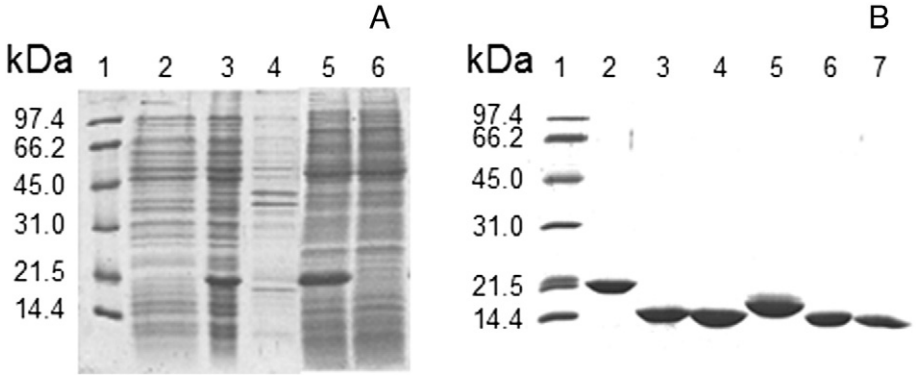

Fig. 1. SDS-PAGE of preS-his and deletion mutant purification steps. (A) The purification steps of preS-his are shown as an example: (1) protein markers; (2) noninduced cells; (3) cells induced with IPTG for 4 h; (4) pellet from cell lysate; (5) supernatant from cell lysate; (6) protein nonretained in the Ni-NTA column. (B) Protein eluted from the column with 10 mM MOPS pH 8.0, 200 mM imidazole. (1) Protein markers; (2) preS-his; (3) $preS_{\Delta1-40}$; (4) $preS_{\Delta20-60}$; (5) $preS_{\Delta40-80}$; (6) $preS_{\Delta60-100}$; (7) $preS_{\Delta80-120}$. The gel was stained with Coomassie blue.

between experimental and theoretical values was the number of methionine residues. In all cases, except for the mutant $preS_{\Delta1-40}$, after acid hydrolysis the methionine content was one residue lower than expected. It is likely that the amino-terminal methionine had been removed by the action of the *E. coli* methionyl amino peptidase except for the mutant $preS_{\Delta1-40}$ where the peptidase seems not to be able to hydrolyze the corresponding Met-Trp peptide bond [32].

3.2. Spectroscopic characterization

The preS domain (subtype ayw) has four tryptophan residues (W32, W41, W66 and W111) and one tyrosine (Y129). Therefore, all deletion mutants will have the tyrosine residue, while the tryptophan content will depend on the deleted sequence, being this number between 2 and 3. Fig. 2 shows the fluorescence emission spectra of preS-his and the different mutant proteins at pH 7.0 which are very similar to those obtained at pH 5.0. The fluorescence emission maximum is centered at 344 nm, regardless of the excitation wavelength, which indicates that the tryptophan residues are found in a relatively polar environment. The contribution of the tyrosine residue to the fluorescence emission is very small, negligible in some cases. This may reflect the lower absorptivity and quantum yield of Tyr compared to Trp although it could also be due to a process of resonance energy transfer from Tyr to the nearby Trp residues or to fluorescence quenching of its neighboring residues in the three dimensional structure of the protein. Nevertheless, the fluorescence intensity at the maximum reflects the lower tryptophan content of mutants $preS_{\Delta20-60}$ and $preS_{\Delta40-80}$.

The far-UV CD spectra of preS-his at pH 7.0 and 5.0 are depicted in Fig. 3A. The shape of the spectra, with a minimum at 200 nm and a shoulder at 220 nm, is indicative of a protein with a high percentage of non-ordered structure. Fig. 3B shows the spectra of the mutant proteins at pH 7.0 that are very similar to those recorded at pH 5.0 in all cases. The assignment of the secondary structure elements according to the algorithm CCA [28] is presented in Table 3. Regardless of pH, the major repetitive ordered secondary structure component is β-sheet (9 to 21%, depending of the mutant protein) and, approximately, a third of the amino acids are in β-turn. It should be noted that 48–59% of the protein has an aperiodic secondary structure and that helical structure is not present.

3.3. Interaction with phospholipids

The interaction of native and mutant preS domains with phospholipids was studied using two approaches. Firstly, the proteins were labeled with NBD-F. Fluorescent labeling of mutant proteins other than $preS_{\Delta1-40}$ resulted in a precipitated sample. Hence, the labeled proteins were denatured with 6 M urea, and then the denaturant agent was removed by exhaustive dialysis against 10 mM MOPS pH 5.0 or 7.0. The far-UV CD spectra of NBD-labeled preS polypeptides were coincident with those of the unlabeled ones. The extent of labeling was calculated from the absorbance spectrum. It was found that all the proteins were labeled approximately in a 1:1 (NBD:protein) ratio. Considering that the reaction was carried out at pH 6.8, it is expected that the α-amino group, and not the Lys side chain, be the main labeling target [33].

It has been previously shown that the interaction of NBD-preS-his protein with neutral phospholipid vesicles is very weak and the binding constant cannot be determined from this type of experiment [23]. Thus, PG vesicles were used to compare the interaction of the mutant proteins with phospholipids. In the absence of phospholipid vesicles, the emission maximum of NBD-labeled proteins was centered at 546 nm, a value similar to that described for other NBD derivatives [29]. Upon

Table 1
Molecular mass and isoelectric point values of preS-his, $preS_{\Delta1-40}$, $preS_{\Delta20-60}$, $preS_{\Delta40-80}$, $preS_{\Delta60-100}$ and $preS_{\Delta80-120}$.

	preS-his	$preS_{\Delta1-40}$	$preS_{\Delta20-60}$	$preS_{\Delta40-80}$	$preS_{\Delta60-100}$	$preS_{\Delta80-120}$
Mr (Da)	18,055	13,843	13,760	14,030	13,984	13,594
pI	8.40	11.34	10.57	8.48	6.78	6.41

Table 2
Amino acid composition of preS-his, $preS_{\Delta1-40}$, $preS_{\Delta20-60}$, $preS_{\Delta40-80}$, $preS_{\Delta60-100}$ and $preS_{\Delta80-120}$.

aa[a]	preS-his	$preS_{\Delta1-40}$	$preS_{\Delta20-60}$	$preS_{\Delta40-80}$	$preS_{\Delta60-100}$	$preS_{\Delta80-120}$
Asx	21 (21)	10 (10)	12 (12)	18 (18)	19 (19)	18 (18)
Thr	12–13 (14)	10 (11)	10 (11)	11 (12)	10 (11)	7 (8)
Ser	11–13 (14)	9–11 (12)	11–13 (14)	11–13 (14)	8 (10)	8 (10)
Glx	11 (11)	9 (9)	11 (11)	8 (8)	6 (6)	6 (6)
Pro	23 (23)	18 (18)	17 (17)	18 (18)	14 (14)	15 (15)
Gly	16 (16)	14 (14)	12 (12)	8 (8)	11 (11)	15 (15)
Ala	13 (13)	10 (10)	7 (7)	8 (8)	10 (10)	11 (11)
Val	4 (4)	4 (4)	3 (3)	3 (3)	4 (4)	4 (4)
Met	1 (2)	2 (2)	1 (2)	1 (2)	1 (2)	0 (1)
Ile	3 (3)	3 (3)	3 (3)	2 (2)	2 (2)	3 (3)
Leu	15 (15)	12 (12)	14 (14)	10 (10)	10 (10)	12 (12)
Tyr	1 (1)	1 (1)	1 (1)	1 (1)	1 (1)	1 (1)
Phe	9 (9)	5 (5)	5 (5)	7 (7)	9 (9)	8 (8)
His	10 (4 + 6)	9 (3 + 6)	9 (3 + 6)	9 (3 + 6)	10 (4 + 6)	8 (2 + 6)
Lys	2 (2)	1 (1)	0 (0)	1 (1)	2 (2)	2 (2)
Arg	7 (7)	6 (6)	6 (6)	7 (7)	5 (5)	4 (4)
Trp	N.D.[b] (4)	N.D. (3)	N.D. (2)	N.D. (2)	N.D. (3)	N.D. (3)

[a] The values in parentheses correspond to the theoretical composition determined from the cDNA sequence.
[b] N.D. (not determined).

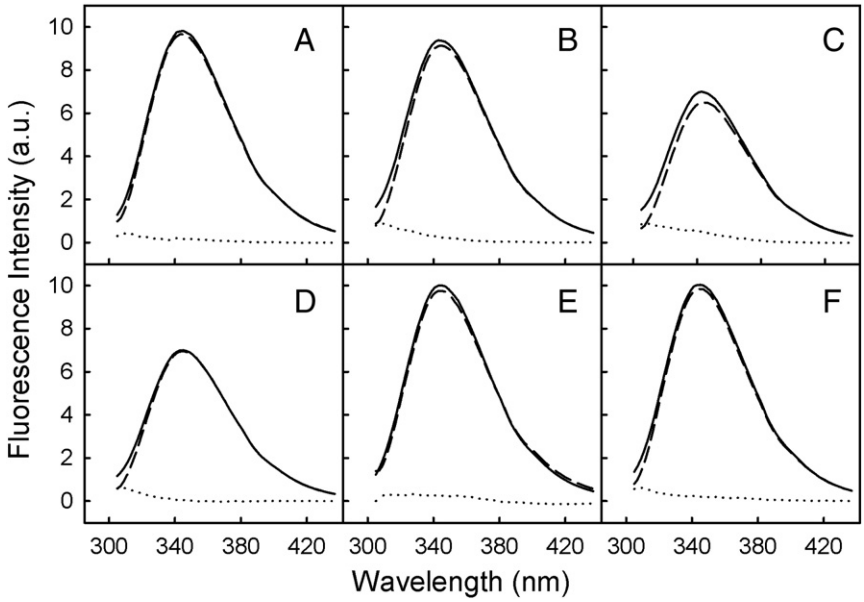

Fig. 2. Fluorescence emission spectra of preS-his (A), $preS_{\Delta 1-40}$ (B), $preS_{\Delta 20-60}$ (C), $preS_{\Delta 40-80}$ (D), $preS_{\Delta 60-100}$ (E) and $preS_{\Delta 80-120}$ (F) at pH 7.0. The spectra were obtained upon excitation at 275 nm (—) and 295 nm (- -). The contribution of tyrosine residues to the emission spectra of the protein (· · · · ·) was calculated as described in the Materials and methods section. Protein concentration was 0.07 mg/mL. The buffer used was 10 mM MOPS pH 7.0. The results shown are representative of those obtained for three different experiments.

interaction with PG vesicles at pH 5.0, the fluorescence intensity increased considerably and the emission maximum was shifted to 522–528 nm (Fig. 4), indicating that the fluorescent probe has been relocated to a more hydrophobic environment. At pH 7.0, the emission maximum shifted to 532 nm and the increase in fluorescence intensity was considerably lower (data not shown). From the fluorescence intensity values observed at pH 5.0 the binding isotherms were plotted (Fig. 5). In the case of the wild-type protein and mutants $preS_{\Delta 1-40}$ and $preS_{\Delta 60-100}$ two different slopes were observed (Fig. 5A, B, E). This behavior has been associated with protein aggregation upon binding to the membrane and the formation of large pores in the vesicles [34]. However, the mutants $preS_{\Delta 40-80}$ and $preS_{\Delta 80-120}$ only have one slope in the binding isotherms (Fig. 5D, F) and $preS_{\Delta 20-60}$ mutant presented a very small difference between the two slopes (Fig. 5C). The partition coefficients, reflecting the binding constants, were calculated as the initial slopes of these binding isotherms (Table 4). In the presence of acidic phospholipids and at pH 5.0, a value between 1.4 and $2.9 \times 10^4\ M^{-1}$ was obtained for all recombinants proteins.

Secondly, circular dichroism was used to ascertain the structural changes which occur in the proteins as the result of their interaction with phospholipid vesicles. The spectra obtained with both preS-his and the different mutants in the presence of PG vesicles are shown in Fig. 6. At pH 5.0 the behavior was very similar for all proteins. Thus, low concentrations of phospholipid (protein:lipid molar ratio of 1:5) produced an increase in ellipticity values, which could be due to aggregation of the proteins on the surface of the bilayer resulting in a lower effective protein concentration. This effect is more pronounced in the case of $preS_{\Delta 60-100}$ and $preS_{\Delta 80-120}$ (Fig. 6, pH 5.0, E–F). Since these two mutants have the lowest isoelectric point of all the recombinant proteins, they would have a lower positive charge that would enable

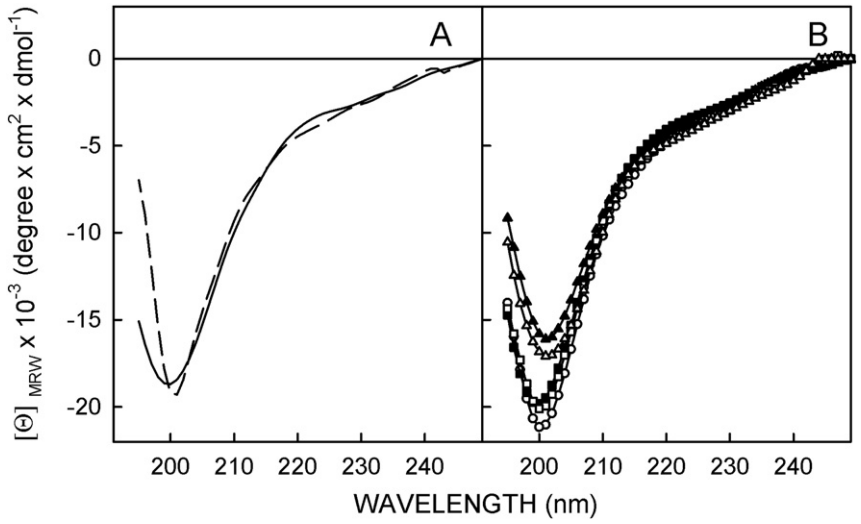

Fig. 3. Circular dichroism spectra of preS-his and mutant proteins. (A) preS-his at pH 5.0 (——) and 7.0 (- - -). (B) Mutants proteins at pH 7.0, $preS_{\Delta 1-40}$ (o), $preS_{\Delta 20-60}$ (■), $preS_{\Delta 40-80}$ (□), $preS_{\Delta 60-100}$ (▲) and $preS_{\Delta 80-120}$ (Δ). Protein concentration was 5 μM and cell path length 0.1 cm. The buffer employed was 10 mM MOPS at the appropriate pH. The results shown are representative of those obtained for three different experiments.

Table 3
Secondary structure of preS-his and mutant proteins calculated from the CD spectra according to the CCA method [28].

Protein	Secondary structure (%)							
	α-Helix		β-Sheet		β-Turn		Aperiodic	
	pH 7.0	pH5.0	pH 7.0	pH5.0	pH 7.0	pH5.0	pH 7.0	pH5.0
preS-his	0	0	18	15	30	32	52	53
$preS_{\Delta 1-40}$	0	0	12	12	34	36	54	52
$preS_{\Delta 20-60}$	0	0	18	9	32	36	50	55
$preS_{\Delta 40-80}$	0	0	18	11	30	30	52	59
$preS_{\Delta 60-100}$	2	0	21	15	29	26	48	59
$preS_{\Delta 80-120}$	3	0	17	17	28	26	52	57

them to interact and form aggregates in a higher proportion. When the phospholipid concentration was increased, protein:lipid molar ratio of 1:20, a shift from 200 nm to 210 nm and the appearance of a shoulder at 225 nm were observed, indicating a conformational change to a secondary structure with a higher content in helical structures. When the concentration of phospholipid was increased to a protein:lipid molar ratio of 1:50, the helical conformation was maintained resulting in a spectrum similar in shape to that observed at a 1:20 molar ratio but with lower ellipticity values, probably due to the presence of a higher proportion of protein in monomeric form. At pH 7.0, the differences between the spectra obtained at 1:20 and 1:50 practically disappeared. As it can be seen in Table 5, where the percentages of the different secondary elements at a protein:lipid molar ratio of 1:50 are shown, although the percentage of non-ordered structure was still high, the percentages of α-helix (14–23%) and β-sheet (16–40%) increased considerably at the expense of β-turn. At pH 7.0, and except for the $preS_{\Delta 1-40}$ mutant, an increase in α-helix concomitant with a decrease in the percentage of extended structure in all cases was observed.

3.4. Vesicle destabilization

The HBV preS domains have been shown to have membrane destabilization properties [23], including the ability to cause vesicle aggregation, lipid mixing and release of aqueous contents. The capability of the deletion mutants to retain these properties was also examined. Vesicle aggregation was followed by measuring the variation of the optical density at 360 nm (ΔOD_{360}) after incubation of PG vesicles at a concentration of 60 μM with different concentrations of protein at 37 °C for 1 h. At pH 7.0, the highest increase in optical density occurs with the wild type protein and $preS_{\Delta 20-60}$, whereas $preS_{\Delta 1-40}$, $preS_{\Delta 40-80}$ and $preS_{\Delta 60-100}$ produced a lower increase and $preS_{\Delta 80-120}$ was not able to induce aggregation (Fig. 7A). However, at pH 5.0 the ΔOD_{360} increased in a concentration dependent manner reaching a maximum at 5.5 μM in all cases (Fig. 7A).

Lipid mixing of phospholipid vesicles was followed by the resonance energy transfer (RET) assay between the fluorescence probes NBD-PE and Rh-PE incorporated into a lipid matrix in which mixing of phospholipids from labeled and unlabeled liposomes resulted in a decrease in energy transfer [30]. Native preS as well as the mutants were able to induce lipid mixing at pH 7.0, although the decrease in energy transfer induced by $preS_{\Delta 100-120}$ was higher at lower concentrations of protein (Fig. 7B). The % RET decreased from 65% in the absence of protein, up to 6.5% for a final protein concentration of 8 μM. These values correspond to a 10-fold dilution in the acceptor surface density, indicating that the complete fusion of vesicles has been induced, since the mere aggregation would not account for this decrease in energy transfer [35]. The same final effect was observed for preS-his and $preS_{\Delta 40-80}$ and $preS_{\Delta 60-100}$ mutants, reaching in all cases the complete fusion of the vesicles. In the case of $preS_{\Delta 1-40}$ and $preS_{\Delta 20-60}$, the % RET only decreases to 29 and 15% respectively (Fig. 7B), probably because vesicle aggregation prevailed over fusion. At pH 5.0 there were no major differences between proteins, leading to a decrease in the % RET to 10% in all cases, which implies the complete fusion of vesicles (Fig. 7B).

The increase in permeability induced by the addition of preS domain and mutant proteins has been studied according to the assay described by Ellens [31]. As described above for aggregation and lipid mixing, the release of aqueous contents is also a protein concentration-dependent process although the maximum effect at pH 7.0 was reached at a protein concentration (0.25–2.0 μM) much lower than that needed to achieve the maximum effect in the other assays (5–8 μM) (Fig. 7C). For the mutant $preS_{\Delta 1-40}$, the maximum effect was reached at the lowest protein concentration (0.2 μM), whereas $preS_{\Delta 40-80}$ and $preS_{\Delta 80-120}$ required a concentration 10 times higher, 2 μM (Fig. 7C). The maximum fluorescence value reached (85–99%) was similar to that described for other

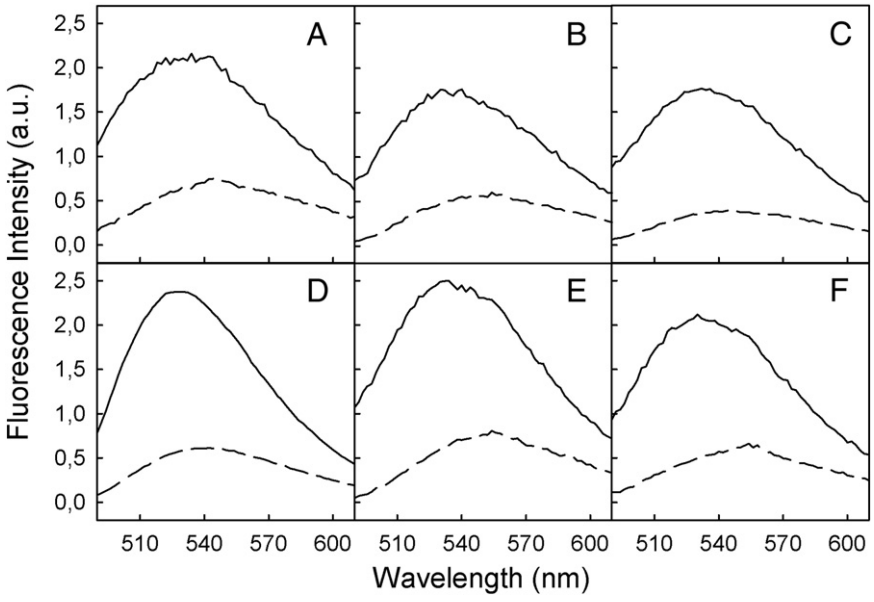

Fig. 4. Fluorescence spectra of NBD-preS-his (A), NBD-$preS_{\Delta 1-40}$ (B), NBD-$preS_{\Delta 20-60}$ (C), NBD-$preS_{\Delta 40-80}$ (D), NBD-$preS_{\Delta 60-100}$ (E) and NBD-$preS_{\Delta 80-120}$ (F). Spectra were measured with an excitation wavelength of 467 nm. The protein concentration used was 0.15–0.20 μM. The spectra of the proteins in the absence (- - -) and presence (—) of lipids at a lipid:protein molar ratio of 5000:1 after incubation of the protein with PG vesicles in medium buffer at pH 5.0 are shown. The results shown are representative of those obtained for three different experiments.

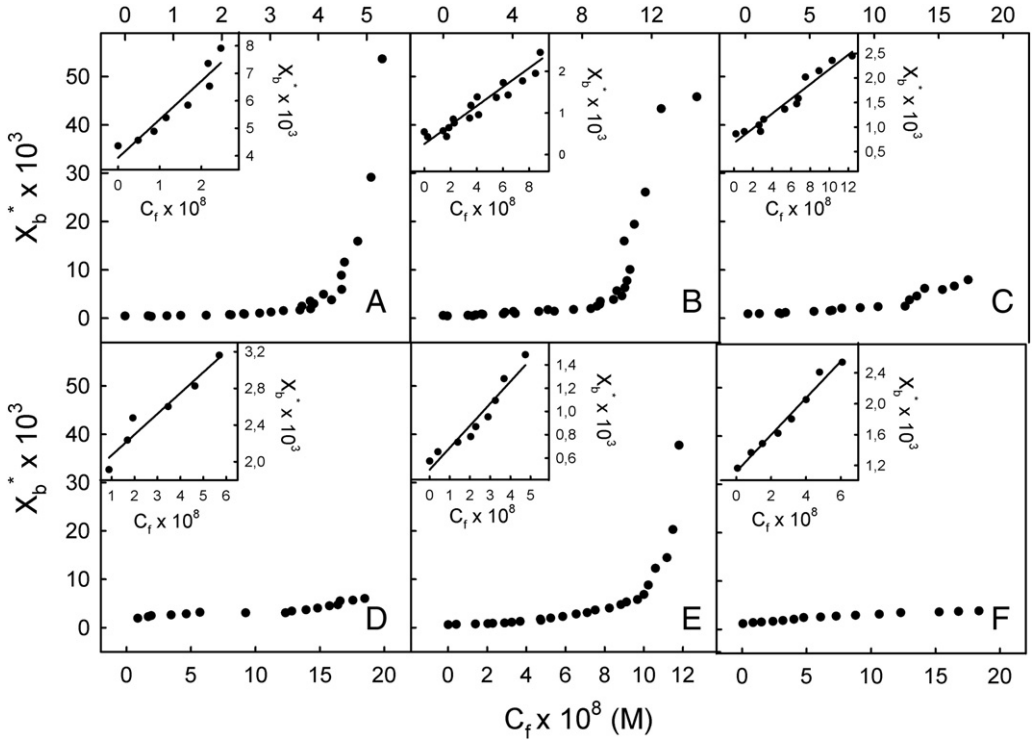

Fig. 5. Binding isotherm of NBD-preS-his (A), NBD-preS$_{\Delta 1-40}$ (B), NBD-preS$_{\Delta 20-60}$ (C), NBD-preS$_{\Delta 40-80}$ (D), NBD-preS$_{\Delta 60-100}$ (E) and NBD-preS$_{\Delta 80-120}$ (F) to PG vesicles at pH 5.0. Values of X_b^* and C_f are calculated from the increments in fluorescence intensity at 530 nm as described in the Materials and methods section. Insets represent the initial slope of the corresponding binding isotherm used to calculate the partition coefficients. The results shown are representative of those obtained for three different experiments.

proteins but lower than the value obtained after the addition of Triton X-100 (100%). At pH 5.0 the behavior of all proteins was nearly identical and in all cases a lower protein concentration is needed to attain the same effect observed at pH 7.0 (Fig. 7C).

4. Discussion

We have previously suggested that different regions of the surface proteins of HBV may be involved in the fusion of viral and cellular membranes [23]. Specifically, the N-terminal portion of the S protein and the preS domains were proposed to contribute at the fusion process either simultaneously or at different stages. To gain information on the location of the region(s) responsible for the destabilizing properties of preS domain we have cloned and purified the preS domain (subtype ayw) and five deletion mutants where a region of 40 amino acids of the preS1 region has been consecutively removed along the sequence of preS (preS$_{\Delta 1-40}$, preS$_{\Delta 20-60}$, preS$_{\Delta 40-80}$, preS$_{\Delta 60-100}$ and preS$_{\Delta 80-120}$). About 15 mg of wild-type protein and 3–6 mg of highly pure mutated protein per liter of culture medium have been obtained.

The spectroscopic characterization of preS domain and deletion mutants was carried out by means of circular dichroism and fluorescence spectroscopy. PreS domain possesses a high percentage of nonordered structure with the different secondary structure elements arranged in an open conformation [26,36,37]. Deconvolution of far-UV circular dichroism spectra shows that the secondary structure of the mutant proteins does not vary significantly with respect to that of the native protein. 48–59% of the residues are in non-regular structure, while β-sheet is the major ordered repetitive structure (9–21%).

PreS domains have the ability to interact with phospholipid vesicles, as indicated by the changes that the fluorescence spectrum of NBD-labeled protein undergoes when challenged by phospholipids [23]. Since the highest effect was observed with acidic phospholipids at pH 5.0, the experiments with the truncated forms were carried out under these conditions. In the presence of PG vesicles at pH 5.0, the fluorescence emission maximum of NBD shifts from 546 to 526–528 nm in all cases. This change reflects a relocation of NBD into a more hydrophobic environment and is comparable to that obtained for peptides which are known to insert deeply into the bilayer [29,34,38,39]. Furthermore, binding isotherms, derived from the increments in fluorescence intensities, provide information about the way in which the interaction occurs [40,41]. The two slopes which are observed in all cases, except preS$_{\Delta 40-80}$ and preS$_{\Delta 80-120}$, are indicative of a high tendency to interact with the lipid bilayer and to form aggregates and pores [34]. The shape of the binding isotherm obtained for preS$_{\Delta 40-80}$ and preS$_{\Delta 80-120}$, with a single slope, could indicate that, at the concentration range studied, the interaction of these mutants occurs in a monomeric form originating small pores. Therefore, it seems that some of the amino acids deleted in these two mutants are necessary for the oligomerization to take place. The partition coefficients, which reflect the binding constant, were calculated from the initial slope of the binding isotherm, resulting in all cases a value of the order of 10^4 M^{-1}, similar to that previously obtained for preS (subtype adw) [23] and duck hepatitis B virus preS domains [24]. They are also very similar to those described in the case of peptides that strongly interact with the bilayer, as is the case of peptides corresponding to the HA protein of influenza virus [42], the internal peptide of Sendai virus [39] and peptides able to form pores therein [29,38].

Table 4
Fluorescence emission maxima and partition coefficients of the interaction of NBD-preS-his, NBD-preS$_{\Delta 1-40}$, NBD-preS$_{\Delta 20-60}$, NBD-preS$_{\Delta 40-80}$, NBD-preS$_{\Delta 60-100}$ and NBD-preS$_{\Delta 80-120}$ with PG vesicles.

Protein	pH	PG emission maxima	K (M^{-1}) × 10^{-4}
NBD-preS-his	7.0	532	0.3 ± 0.1
	5.0	522	2.9 ± 0.7
NBD-preS$_{\Delta 1-40}$	5.0	526	1.8 ± 0.5
NBD-preS$_{\Delta 20-60}$	5.0	528	1.7 ± 0.2
NBD-preS$_{\Delta 40-80}$	5.0	523	2.4 ± 0.5
NBD-preS$_{\Delta 60-100}$	5.0	528	2.8 ± 0.7
NBD-preS$_{\Delta 80-120}$	5.0	528	1.4 ± 0.8

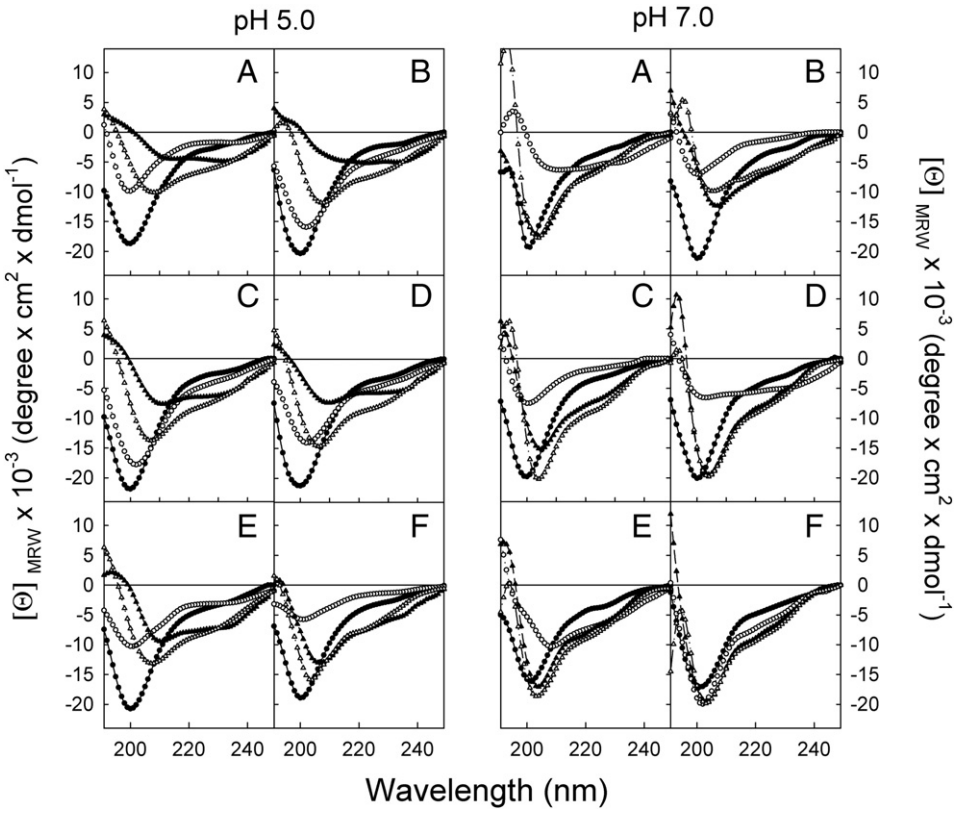

Fig. 6. CD spectra of preS-his (A) and $preS_{\Delta 1-40}$ (B), $preS_{\Delta 20-60}$ (C), $preS_{\Delta 40-80}$ (D), $preS_{\Delta 60-100}$ (E) and $preS_{\Delta 80-120}$ (F) in the presence of PG. The spectra were measured after incubation of the protein in 10 mM MOPS pH 5.0 or 7.0 with different concentrations of the phospholipid for 1 h at 37 °C. The protein concentration was 5 μM. Protein in solution (●) and protein in the presence of PG at a protein:lipid molar ratio of 1:5 (o), 1:20 (▲) and 1:50 (Δ). The results shown are representative of those obtained for three different experiments.

Interaction with liposomes also established structural alterations in the preS domains and mutant proteins. CD spectra obtained in the presence of acidic phospholipid vesicles show that at low concentrations of phospholipid the value of the molar ellipticity increases in all cases, more at pH 7.0 and at pH 5.0 for $preS_{\Delta 60-100}$ and $preS_{\Delta 80-120}$. Under these conditions, and given the low lipid concentration, an increase in the surface density of proteins in the bilayer could favor its aggregation and hence, a higher local concentration of chromophores which could promote a decrease in absorption [43,44]. This aggregation effect is transient because when the concentration of phospholipid increases a reduction in the ellipticity values is noticed. In this regard, it was found that the carboxy- and amino-terminal heptad region of the fusion protein of Sendai virus form complexes in solution [45] which then dissociate into monomers when they bind to the membranes [46]. A similar effect has been described for HIV [47]. As a result of the interaction with acidic phospholipids, from a protein:lipid molar ratio of 1:20 and both at pH 7.0 and 5.0, there is a conformational change of the protein that resulted in an increase of the percentage of helical content, that is very similar in all cases, except for $preS_{\Delta 80-120}$ mutant at pH 7.0, which retain a high content of non-ordered structures. As indicated above, the results obtained with the domains labeled with NBD point to the insertion of the amino-terminal end of the protein into the bilayer. In this sense, myristoylation of the Gly2 residue of the preS domain [3] would help this region to insert. Thus, it seems reasonable to think that the conformational transition to a helical structure occurs in this area, remaining the rest of the protein at the polar surface, maintaining its original structure. As it has been reported in other fusogenic viral proteins, such as the hemagglutinin influenza virus [48,49] or the vesicular stomatitis virus [50], preS domains not only interact with but also are able to destabilize model membrane systems. Both native and mutant proteins have destabilizing properties (aggregation, lipid mixing and release of aqueous contents) in a pH-dependent manner, with the effects observed at pH 5.0 higher than those obtained at neutral pH, especially at low protein concentration. Aggregation results at pH 7.0 are those which provide greater differences between the recombinant proteins. According to these results, the region 20–60 is completely dispensable since the mutant $preS_{\Delta 20-60}$ gives comparable results to those obtained with full length preS domain. Similarly, the 1–40 region seems not to have any involvement in the interactions that promote vesicle aggregation. However, any of the other areas that are missing in the other three mutants would be required for the establishment of such interactions, especially the regions 40–80 and 80–120. The differences could be explained on the basis of the net charge of the protein at pH 7.0. The mutants $preS_{\Delta 60-100}$ and $preS_{\Delta 80-120}$ that have a similar isoelectric point, 6.78 and 6.41 respectively (Table 1) would have the same behavior. However, $preS_{\Delta 80-120}$ is not able to induce aggregation, while $preS_{\Delta 60-100}$ induces vesicle aggregation to the same level than the mutant $preS_{\Delta 1-40}$, which is the one with the highest positive charge at neutral pH (pI 11.34). It is therefore clear that ionic interactions are important in determining the aggregation but there must be

Table 5
Secondary structure of preS-his and mutant proteins in the presence of PG at a protein/lipid molar ratio of 1:50 calculated from the CD spectra according to the CCA method [28].

Protein	Secondary structure (%)							
	α-Helix		β-Sheet		β-Turn		Aperiodic	
	pH 7.0	pH 5.0	pH 7.0	pH 5.0	pH 7.0	pH 5.0	pH 7.0	pH 5.0
preS-his	16	17	6	40	30	8	48	35
$preS_{\Delta 1-40}$	17	22	35	32	16	10	32	36
$preS_{\Delta 20-60}$	24	23	0	26	27	10	49	41
$preS_{\Delta 40-80}$	22	22	0	25	28	8	50	45
$preS_{\Delta 60-100}$	18	22	5	30	23	7	54	41
$preS_{\Delta 80-120}$	19	14	2	16	25	22	54	48

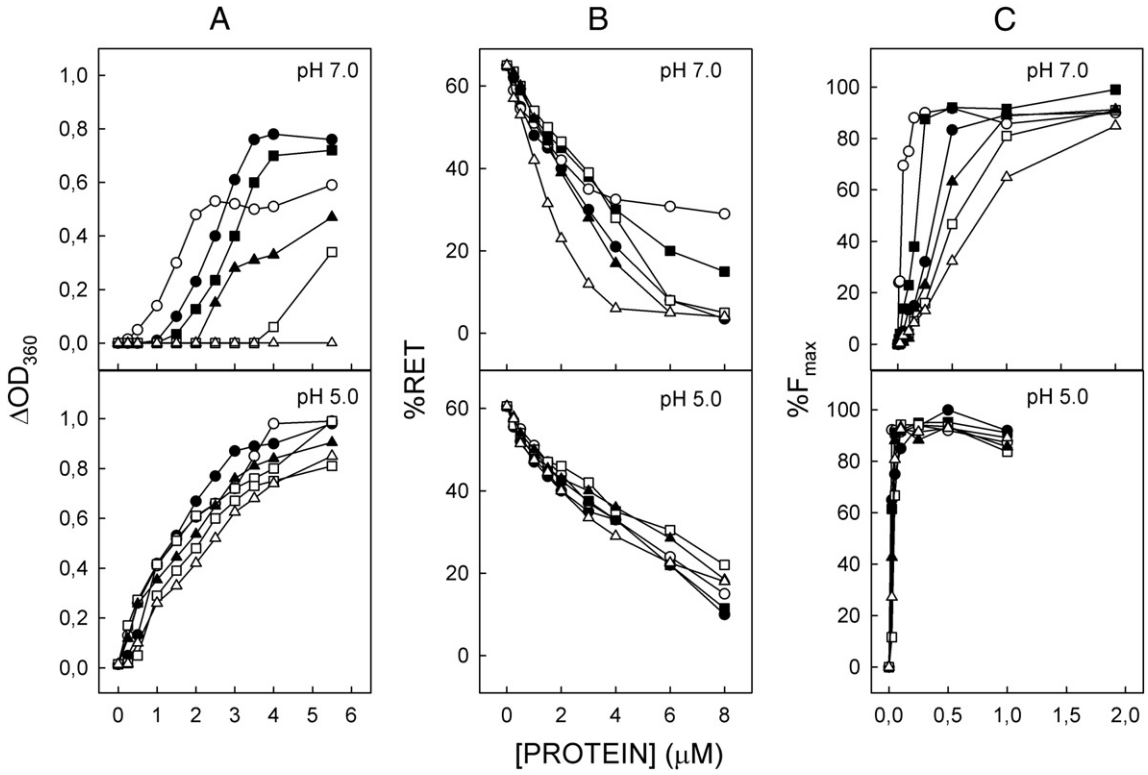

Fig. 7. Aggregation (A), lipid mixing (B) and leakage (C) of PG vesicles induced at pH 7.0 and 5.0 by preS-his (●), $preS_{\Delta1-40}$ (○), $preS_{\Delta20-60}$ (■), $preS_{\Delta40-80}$ (□), $preS_{\Delta60-100}$ (▲) and $preS_{\Delta80-120}$ (△). The final phospholipid concentration was 60 μM (A) and 0.14 mM (B and C). The results shown are representative of those obtained for at least three different experiments. (A) The increase in optical density at 360 nm (ΔOD_{360}) was measured after incubation of the vesicles with the proteins at different concentrations. Values of control samples containing only PG liposomes were subtracted. (B) Increasing concentrations of the different proteins were added to a 1:9 mixture of labeled (NBD-PE 1% and Rh-PE 1%) and unlabeled PG vesicles hydrated in medium buffer. (C) Increasing concentrations of the different proteins were added to PG vesicles loaded with ANTS and DPX. The $\%F_{max}$ was calculated with respect the value obtained upon addition of 0.5% Triton X-100. F.

some additional factors which are also important. As indicated above by the results of the interaction studies with NBD-labeled proteins, $preS_{\Delta40-80}$ and $preS_{\Delta80-120}$ are the mutants that interact with lipid bilayers in a monomeric way. The rest of mutants and the wild type protein induce aggregates that can give rise to an extensive network of vesicles, interacting among themselves, that would account for the increase in optical density at 360 nm. The fact that $preS_{\Delta60-100}$ can form oligomers and induce aggregation, like the rest of mutants, is indicative that the regions responsible for this effect are located between amino acids 40–60 and 100–120.

The inability of mutant $preS_{\Delta40-80}$ and $preS_{\Delta80-120}$ to form aggregates upon interaction with phospholipids could explain their reduced ability to induce release of aqueous contents, since the absence of such complexes has been also related to the formation of smaller pores on the membrane [29]. On the other hand, interaction in a monomeric way may also facilitate the diffusion of NBD-PE and Rh-PE molecules in the fused vesicles, allowing the $preS_{\Delta80-120}$ mutant to induce lipid mixing more efficiently. In contrast, $preS_{\Delta1-40}$ and $preS_{\Delta20-60}$, with a greater capacity to form protein aggregates on the bilayer, are those that produce the greatest vesicle aggregation and release of aqueous contents. In this regard, it has been postulated that oligomerization is necessary for the oblique insertion of fusogenic peptides in the membrane, a condition which strongly promotes fusion [51–53].

Special attention must be paid to the results obtained with mutants $preS_{\Delta1-40}$ and $preS_{\Delta20-60}$. These proteins have a greater ability to destabilize lipid vesicles, both at pH 7.0 and pH 5.0 and at lower protein concentration, than the wild type protein. This could indicate that the first 60 amino acids are not required to initiate the fusion process. This region has been related to the interaction with the receptor and to the species specificity [3,13]. In addition, the region between amino acids 47 and 67 is the most hydrophobic of the preS domain with a hydrophobicity index of 0.7 (Fig. 8), and could be responsible for the insertion of the preS domain in lipid bilayer. Indeed, it possesses the characteristic of a transmembrane helix and also the Gly-X-Phe sequence characteristic of fusogenic peptides, present in the influenza virus and in a reversed form at the amino-terminal of the fusogenic peptide of paramyxovirus, in the center of retrovirus and S domain of HBV [54]. It is also a highly conserved domain among the different HBV subtypes (Fig. 9A) and has sequence homology with fusogenic peptides of viruses such as HIV (Fig. 9B). However, as noted above, this area does not appear to be necessary in the mutants to destabilize lipid vesicles.

All the differences between the mutant proteins disappear at acidic pH and high protein concentration. This could be related to the higher positive charge of all the mutants at lower pH. Anyway, it is clear that all of the mutants, to a greater or lesser extent, may interact with acidic phospholipid and display all the properties assigned to fusogenic proteins. These data would indicate that there is no a specific region of the protein responsible for the fusion of viral and cellular membranes. Like other viruses, such as paramyxoviruses, where there are no sequence homologies between them [55,56], it is the tridimensional structure of the fusogenic peptides what determines the ability to destabilize vesicles and not the amino acid sequence [57,58]. In this regard, the CD spectra indicate that both the full-length protein and the mutants have a similar secondary structure. Moreover, the hydrophobicity profiles indicate that all the proteins share a similar distribution of polar and nonpolar amino acids (Fig. 8). Since all proteins used in this study share the carboxyl-terminal region, which corresponds to the preS2 domain, this area could be responsible for the ionic interaction with the polar head of the phospholipids. Then, the preS1 domain could insert into the bilayer causing its destabilization due to the fact that there is a particular three dimensional structure and/or a distribution of specific amino acids.

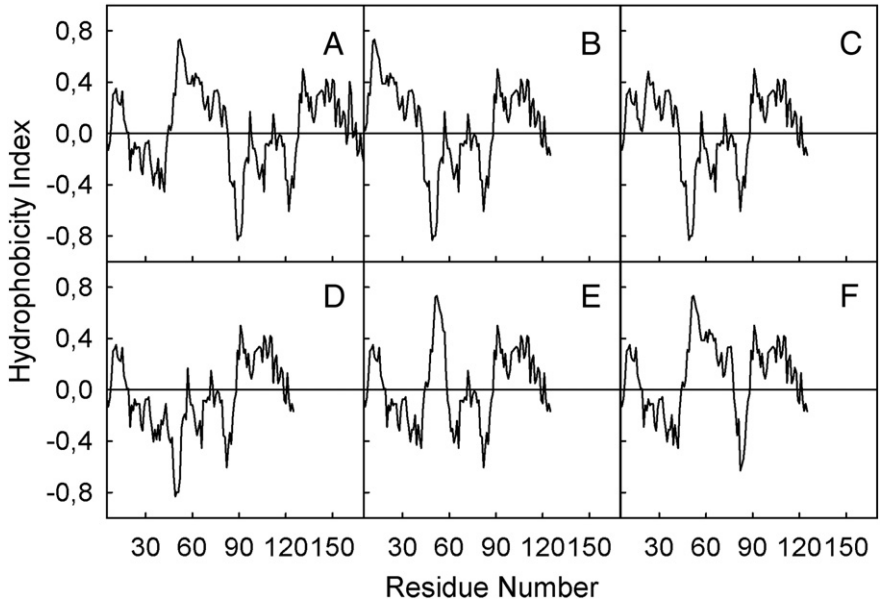

Fig. 8. Hydrophobicity profile of preS-his (A) and mutants $preS_{\Delta 1-40}$ (B), $preS_{\Delta 20-60}$ (C), $preS_{\Delta 40-80}$ (D), $preS_{\Delta 60-100}$ (E) and $preS_{\Delta 80-120}$ (F). The hydrophobicity index was calculated according to the scale proposed by Eisenberg [60].

We have previously proposed that both the N-terminal region of the S protein as well as the preS domains may be involved in the initial steps of viral infection [23]. Thus, antibodies elicited against both regions may play an important role in controlling the infection. Although this study shows that the first 60 amino acids of preS do not seem to be involved in the interaction and destabilization of lipid bilayers, and since it has

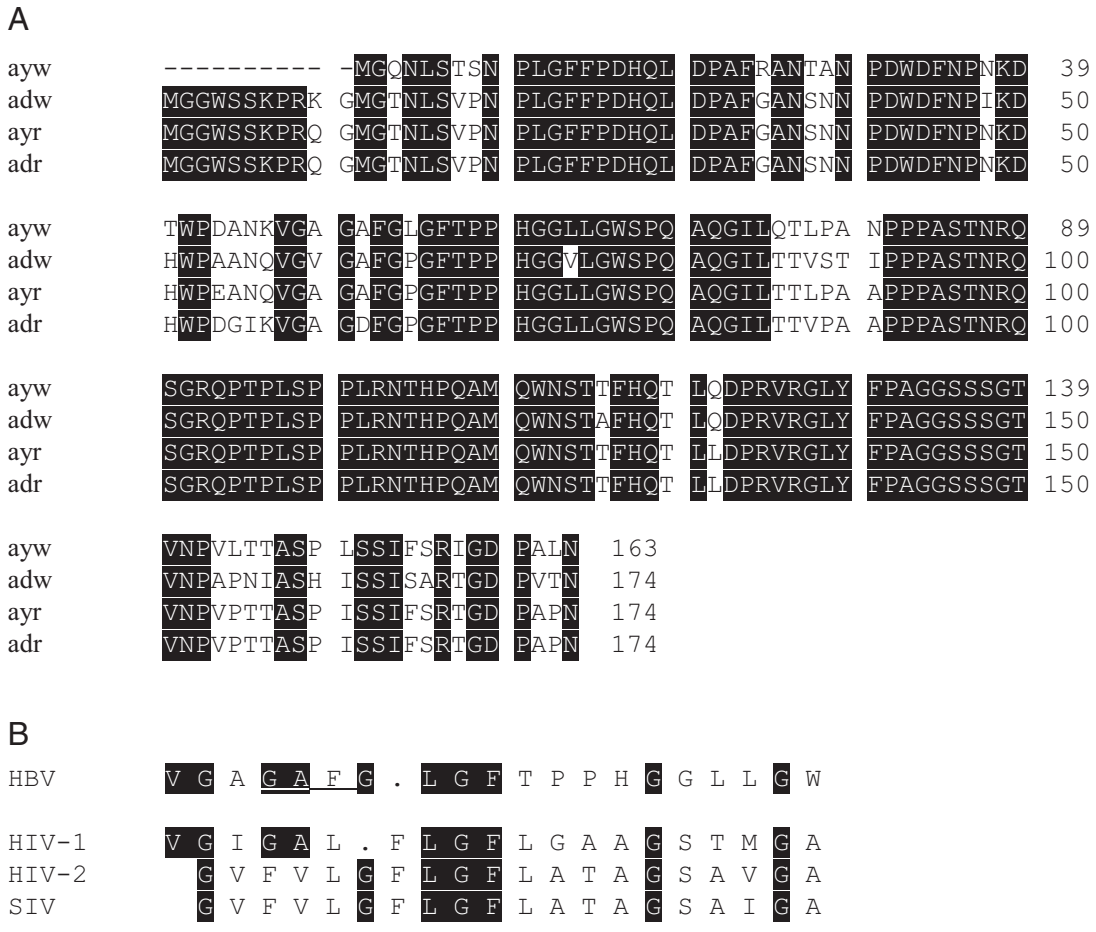

Fig. 9. Amino acid sequence of the preS domains of different HBV subtypes (A). Comparison of positions 47–66 of preS (ayw) with different retrovirus fusogenic peptides (B). The sequence GXF found in other fusogenic peptides is underlined. Sequence identities are shown in black boxes.

been shown that this region is important for the infectivity [3] the use of full-length preS domains as part of a vaccine against HBV infection seems appropriate. In fact, it has been reported an increase in antibody response to a vaccine containing both preS1 and preS2 even in a population that include low responders to the conventional vaccine [59]. Also, there is a phase II clinical trials in chronic HBV-infected patients with a vaccine including preS-derived peptides [2].

Acknowledgements

This work was supported by Grant BFU2010-22014 from the Ministerio de Economía y Competitividad (Spain).

References

[1] J.J. Ott, G.A. Stevens, J. Groeger, S.T. Wiersma, Global epidemiology of hepatitis B virus infection: new estimates of age-specific HBsAg seroprevalence and endemicity, Vaccine 30 (2012) 2212–2219.
[2] T.F. Baumert, L. Meredith, Y. Ni, D.J. Felmlee, J.A. McKeating, S. Urban, Entry of hepatitis B and C viruses — recent progress and future impact, Curr. Opin. Virol. 4 (2014) 58–65.
[3] D. Glebe, C.M. Bremer, The molecular virology of hepatitis B virus, Semin. Liver Dis. 33 (2013) 103–112.
[4] A.R. Neurath, S.B. Kent, N. Strick, P. Taylor, C.E. Stevens, Hepatitis B virus contains pre-S gene-encoded domains, Nature 315 (1985) 154–156.
[5] A.R. Neurath, S.B.H. Kent, N. Strick, K. Parker, Identification and chemical synthesis of a host cell receptor binding site on hepatitis B virus, Cell 46 (1986) 429–436.
[6] A.R. Neurath, B. Seto, N. Strick, Antibodies to synthetic peptides from the preS1 region of the hepatitis B virus (HBV) envelope (env) protein are virus-neutralizing and protective, Vaccine 7 (1989) 234–236.
[7] P. Pontisso, M.G. Ruvoletto, W.H. Gerlich, K.-H. Heermann, R. Bardini, A. Alberti, Identification of an attachment site for human liver plasma membranes on hepatitis B virus particles, Virology 173 (1989) 522–530.
[8] P. Pontisso, M.A. Petit, M.J. Bankowski, M.E. Peeples, Human liver plasma membranes contain receptors for the hepatitis B virus pre-S1 region and, via polymerized human serum albumin, for the pre-S2 region, J. Virol. 63 (1989) 1981–1988.
[9] N. Paran, B. Geiger, Y. Shaul, HBV infection of cell culture: evidence for multivalent and cooperative attachment, EMBO J. 20 (2001) 4443–4453.
[10] J. Le Seyec, P. Chouteau, I. Cannie, C. Guguen-Guillouzo, P. Gripon, Infection process of the hepatitis B virus depends on the presence of a defined sequence in the preS1 domain, J. Virol. 73 (1999) 2052–2057.
[11] P. Chouteau, J. Le Seyec, I. Cannie, M. Nassal, C. Guguen-Guillouzo, P. Gripon, A shot N-proximal region in the large envelope protein harbors a determinant that contributes to the species specificity of human hepatitis B virus, J. Virol. 75 (2001) 11565–11572.
[12] S. De Meyer, Z.J. Gong, W. Suwandhi, J. Van Pelt, A. Soumillion, S.H. Yap, Organ and species specificity of hepatitis B virus (HBV) infection: a review of literature with a special reference to preferential attachment of HBV to human hepatocytes, J. Viral Hepat. 4 (1997) 145–153.
[13] D. Glebe, S. Urban, Viral and cellular determinants involved in hepadnaviral entry, World J. Gastroenterol. 13 (2007) 22–38.
[14] A. Meier, S. Mehrle, T.S. Weiss, W. Mier, S. Urban, Myristoylated PreS1-domain of the hepatitis B virus L-protein mediates specific binding to differentiated hepatocytes, Hepatology 58 31-42.
[15] U. Treichel, K.H. Meyer zum Büschenfelde, H.P. Dienes, G. Gerken, Receptor-mediated entry of hepatitis B into liver cells, Arch. Virol. 142 (1997) 493–498.
[16] S. De Falco, M.G. Ruvoletto, A. Verdoliva, M. Ruvo, A. Raucci, M. Marino, S. Senatore, G. Cassani, A. Alberti, P. Pontisso, G. Fassina, Cloning and expression of a novel hepatitis B virus-binding protein from HepG2 cells, J. Biol. Chem. 276 (2001) 36613–36623.
[17] H. Jeulin, A. Velay, J. Murray, E. Schvoerer, Clinical impact of hepatitis B and C virus envelope glycoproteins, World J. Gastroenterol. 19 (2014) 654–664.
[18] H. Yan, G. Zhong, G. Xu, W. He, Z. Jing, Z. Gao, Y. Huang, Y. Qi, B. Peng, H. Wang, L. Fu, M. Song, P. Chen, W. Gao, B. Ren, Y. Sun, T. Cai, X. Feng, J. Sui, W. Li, Sodium taurocholate cotransporting polypeptide is a functional receptor for human hepatitis B and D virus, Elife 1 (2012) e00049 (Cambridge).
[19] I. Rodríguez-Crespo, E. Núñez, J. Gómez-Gutierrez, B. Yélamos, J.P. Albar, D.L. Peterson, F. Gavilanes, Phospholipid interactions of a putative fusion peptide of hepatitis B virus surface antigen S protein, J. Gen. Virol. 76 (1995) 301–308.
[20] I. Rodríguez-Crespo, J. Gómez-Gutiérrez, J.A. Encinar, J.M. Gónzalez-Ros, J.P. Albar, D.L. Peterson, F. Gavilanes, Structural properties of the putative fusion peptide of hepatitis B virus upon interaction with phospholipids. Circular dichroism and Fourier-transform infrared spectroscopy studies, Eur. J. Biochem. 242 (1996) 243–248.
[21] X. Lu, T. Hazboun, T. Block, Limited proteolysis induces woodchuck hepatitis virus infectivity for human HepG2 cells, Virus Res. 73 (2001) 27–40.
[22] C. Maenz, S.F. Chang, A. Iwanski, M. Bruns, Entry of duck hepatitis B virus into primary duck liver and kidney cells after discovery of a fusogenic region within the large surface protein, J. Virol. 81 (2007) 5014–5023.
[23] E. Núñez, B. Yélamos, C. Delgado, J. Gómez-Gutiérrez, D.L. Peterson, F. Gavilanes, Interaction of preS domains of hepatitis B virus with phospholipid vesicles, Biochim. Biophys. Acta 17884 (2009) 417–424.
[24] C.L. Delgado, E. Nunez, B. Yelamos, J. Gomez-Gutierrez, D.L. Peterson, F. Gavilanes, Spectroscopic characterization and fusogenic properties of preS domains of duck hepatitis B virus, Biochemistry (Mosc) 51 (2012) 8444–8454.
[25] Y. Ni, J. Sonnabend, S. Seitz, S. Urban, The pre-s2 domain of the hepatitis B virus is dispensable for infectivity but serves a spacer function for L-protein-connected virus assembly, J. Virol. 84 (2010) 3879–3888.
[26] E. Núñez, X. Wei, C. Delgado, I. Rodríguez-Crespo, B. Yélamos, J. Gómez-Gutiérrez, D.L. Peterson, F. Gavilanes, Cloning, expression, and purification of histidine-tagged preS domains of hepatitis B virus, Protein Expr. Purif. 21 (2001) 183–191.
[27] R.J. Pogulis, A.N. Vallejo, L.R. Pease, In vitro recombination and mutagenesis by overlap extension PCR, Methods Mol. Biol. 57 (1996) 167–176.
[28] A. Perczel, M. Hollósi, G. Tusnády, G.D. Fasman, Deconvolution of the circular dichroism spectra of proteins: the circular dichroism spectra of antiparallel b-sheet in proteins, Protein Eng. 4 (1991) 669–679.
[29] D. Rapaport, Y. Shai, Interaction of fluorescently labeled pardaxin and its analogues with lipid bilayers, J. Biol. Chem. 266 (1991) 23769–23775.
[30] D.K. Struck, D. Hoekstra, R.E. Pagano, Use of resonance energy transfer to monitor membrane fusion, Biochemistry (Mosc) 20 (1981) 4093–4099.
[31] H. Ellens, J. Bentz, F.C. Szoka, H^+- and Ca^{2+}-induced fusion and destabilization of liposomes, Biochemistry (Mosc) 24 (1985) 3099–3106.
[32] P.H. Hirel, M.J. Schmitter, P. Dessen, G. Fayat, S. Blanquet, Extent of N-terminal methionine excision from *Escherichia coli* proteins is governed by the side-chain length of the penultimate amino acid, Proc. Natl. Acad. Sci. U. S. A. 86 (1989) 8247–8251.
[33] K. Rajarathnam, J. Hochman, M. Schindler, S. Ferguson-Miller, Synthesis, location, and lateral mobility of fluorescently labeled ubiquinone 10 in mitochondrial and artificial membranes, Biochemistry (Mosc) 28 (1989) 3168–3176.
[34] D. Rapaport, Y. Shai, Interaction of fluorescently labeled analogues of the amino-terminal fusion peptide of Sendai virus with phospholipid membranes, J. Biol. Chem. 269 (1994) 15124–15131.
[35] R. Blumenthal, M. Henkart, C.J. Steer, Clathrin-induced pH-dependent fusion of phosphatidylcholine vesicles, J. Biol. Chem. 258 (1983) 3409–3415.
[36] S. Delos, M.T. Villar, P. Hu, D.L. Peterson, Cloning, expression, isolation and characterization of the pre-S domains of hepatitis B surface antigen, devoid of the S protein, Biochem. J. 276 (1991) 411–416.
[37] C.-Y. Maeng, M.S. Oh, I.H. Park, H.J. Hong, Purification and structural analysis of the hepatitis B virus preS1 expressed from *Escherichia coli*, Biochem. Biophys. Res. Commun. 282 (2001) 787–792.
[38] Y. Pouny, D. Rapaport, A. Mor, P. Nicolas, Y. Shai, Interaction of antimicrobial dermaseptin and its fluorescently labeled analogues with phospholipid membranes, Biochemistry (Mosc) 31 (1992) 12416–12423.
[39] J.K. Ghosh, S.G. Peisajovich, Y. Shai, Sendai virus internal fusion peptide: structural and functional characterization and a plausible mode of viral entry inhibition, Biochemistry (Mosc) 39 (2000) 11581–11592.
[40] G. Schwarz, S. Stankowski, V. Rizzo, Thermodynamic analysis of incorporation and aggregation in a membrane: application to the pore-forming peptide alamethicin, Biochim. Biophys. Acta 861 (1986) 141–151.
[41] G. Schwarz, H. Gerke, V. Rizzo, S. Stankowski, Incorporation kinetics in a membrane, studied with the pore-forming peptide alamethicin, Biophys. J. 52 (1987) 685–692.
[42] X. Han, L.K. Tamm, pH-dependent self-association of influenza hemagglutinin fusion peptides in lipid bilayers, J. Mol. Biol. 304 (2000) 953–965.
[43] L. Horniak, M. Pilon, R. van't Hof, B. de Kruijff, The secondary structure of the ferredoxin transit sequence is modulated by its interaction with negatively charged lipids, FEBS Lett. 334 (1993) 241–246.
[44] I. Lackzó, M. Hollòsi, E. Uass, G. Toth, Liposome-induction conformational changes of an epitopic peptide and its palmitoylated derivative of influenza virus hemagglutinin, Biochem. Biophys. Res. Commun. 249 (1998) 213–217.
[45] J.K. Ghosh, Y. Shai, A peptide derived from a conserved domain of Sendai Virus fusion protein inhibits virus–cell fusion, J. Biol. Chem. 273 (1998) 7252–7259.
[46] I. Ben-Efraim, Y. Kliger, C. Hermesh, Y. Shai, Membrane-induced step in the activation of Sendai virus fusion protein, J. Mol. Biol. 285 (1999) 609–625.
[47] N.C. Santos, M. Priteo, M.A.R.B. Castanho, Interaction of the major epitope region of HIV-1 protein gp41 with membrane model systems. A fluorescence spectroscopy study, Biochemistry (Mosc) 37 (1998) 8674–8682.
[48] J. Ramalho-Santos, S. Nir, N. Duzgunes, A.P. de Carvalho, C. de Lima Mda, A common mechanism for influenza virus fusion activity and inactivation, Biochemistry (Mosc) 32 (1993) 2771–2779.
[49] L.V. Chernomordik, E. Leikina, V. Frolov, P. Bronk, J. Zimmerberg, An early stage of membrane fusion mediated by the low pH conformation of influenza hemagglutinin depends upon membrane lipids, J. Cell Biol. 136 (1997) 81–93.
[50] A. Puri, M. Krumbiegel, D. Dimitrov, R. Blumenthal, A new approach to measure fusion activity of cloned viral envelope proteins: fluorescence dequenching of octadecylrhodamine-labeled plasma membrane vesicles fusing with cells expressing vesicular stomatitis virus glycoprotein, Virology 195 (1993) 855–858.
[51] R. Brasseur, T. Pillot, L. Lins, J. Vandekerckhove, M. Rosseneu, Peptides in membranes: tipping the balance of membrane stability, Trends Biochem. Sci. 22 (1997) 167–171.
[52] E.-I. Pécheur, J. Sainte-Marie, A. Bienvenüe, D. Hoekstra, Membrane fusion induced by 11-mer anionic and cationic peptides: a structure–function study, Biochemistry (Mosc) 37 (1998) 2361–2371.
[53] E.-I. Pécheur, J. Sainte-Marie, A. Bienvenüe, D. Hoekstra, Lipid headgroup spacing and peptide penetration, but not peptide oligomerization, modulate peptide-induced fusion, Biochemistry (Mosc) 38 (1999) 364–373.

[54] E.I. Pécheur, J. Sainte-Marie, A. Bienvenüe, D. Hoekstra, Peptides and membrane fusion: towards an understanding of the molecular mechanism of protein-induced fusion, J. Membr. Biol. 167 (1999) 1–17.
[55] S.R. Durell, I. Martin, J.-M. Ruysschaert, Y. Shai, R. Blumenthal, What studies of fusion peptides tell us about viral envelope glycoprotein-mediated membrane fusion (review), Mol. Membr. Biol. 14 (1997) 97–112.
[56] O. Samuel, Y. Shai, Participation of two fusion peptides in measles virus-induced membrane fusion: emerging similarity with other paramyxoviruses, Biochemistry (Mosc) 40 (2001) 1340–1349.
[57] I. Callebaut, A. Tasso, R. Brasseur, A. Burny, D. Portetelle, J.P. Mornon, Common prevalence of alanine and glycine in mobile reactive centre loops of serpins and viral fusion peptides: do prions possess a fusion peptide? J. Comput. Aided Mol. Des. 8 (1994) 175–191.
[58] S.M. Davies, R.F. Epand, J.P. Bradshaw, R.M. Epand, Modulation of lipid polymorphism by the feline leukemia virus fusion peptide: implications for the fusion mechanism, Biochemistry (Mosc) 37 (1998) 5720–5729.
[59] P. Rendi-Wagner, D. Shouval, B. Genton, Y. Lurie, H. Rumke, G. Boland, A. Cerny, M. Heim, D. Bach, M. Schroeder, H. Kollaritsch, Comparative immunogenicity of a PreS/S hepatitis B vaccine in non- and low responders to conventional vaccine, Vaccine 24 (2006) 2781–2789.
[60] D. Eisenberg, E. Schwarz, M. Komaromy, R. Wall, Analysis of membrane and surface protein sequences with the hydrophobic moment plot, J. Mol. Biol. 179 (1984) 125–142.